Supplementary Data

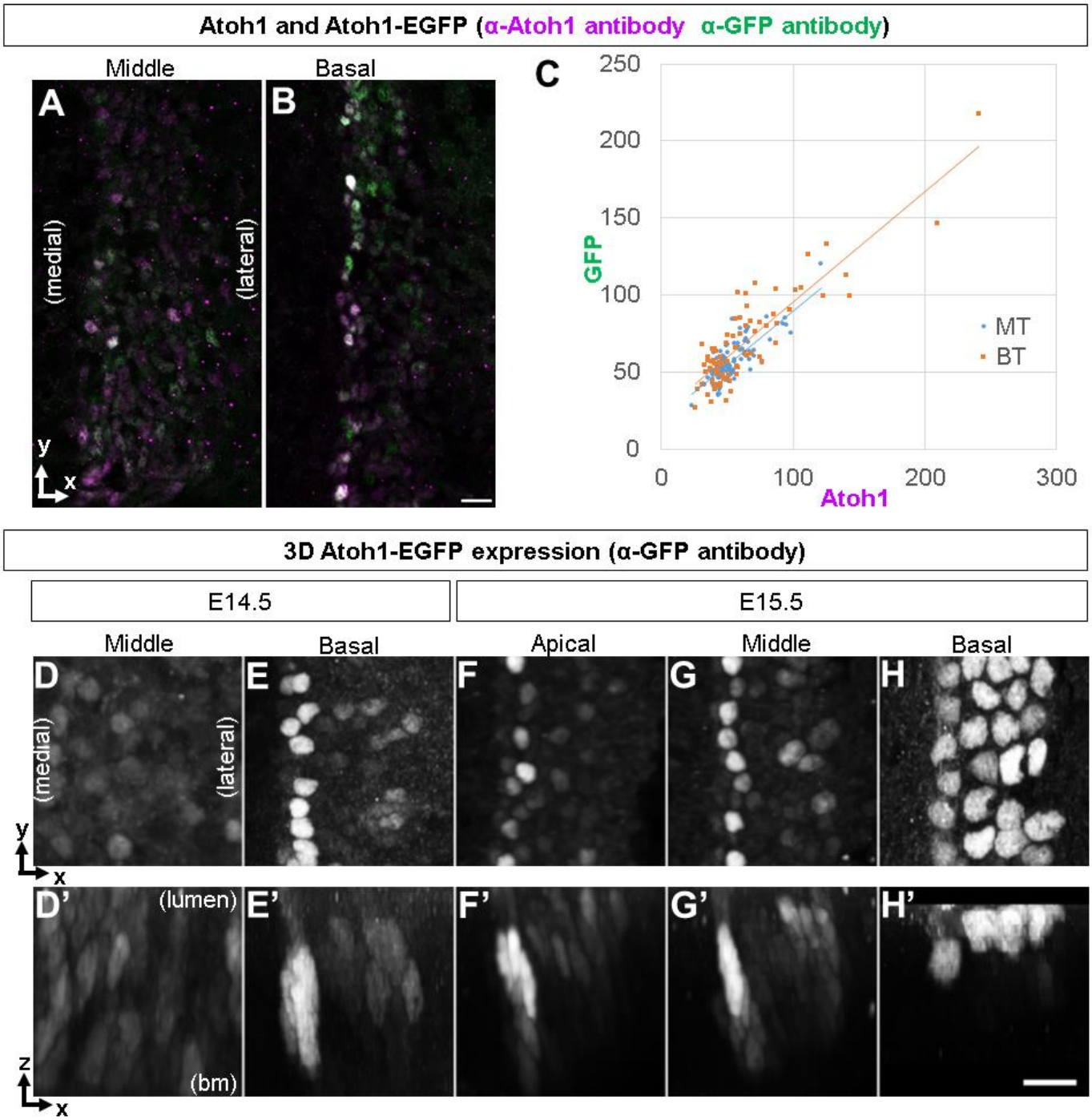

Fig. S1. GFP intensity in prosensory cells of cochleae of *Atoh1*-EGFP mouse embryos can be interpreted as representative of endogenous Atoh1 levels.

(A-C) Comparison of *Atoh1*-EGFP with endogenous Atoh1 expression.

We carried out an immunohistochemical analysis of *Atoh1*-EGFP in the cochlear epithelium of E14.5 embryos using both anti-GFP and anti-Atoh1 antibodies.

(A, B) Atoh1 and GFP expression in the middle turn (A) and basal turn (B) of E14.5 *Atoh1*-EGFP cochlear epithelium visualized by anti-GFP (green) and anti-Atoh1 (magenta) antibody. In prosensory cells, weak, diffuse and salt-and-pepper staining was detected by both anti-GFP and anti-Atoh1 antibodies.

Scale bar: a and b, 10 μm.

(C) Relative expression intensity of Atoh1 and GFP in individual GFP-positive cells of E14.5 *Atoh1*-EGFP cochlear epithelium. A significant positive linear correlation was observed between relative GFP intensity and relative Atoh1 intensity (MT, $r = 0.787$; BT, $r = 0.877$, $p < 0.01$). MT, middle turn; BT, basal turn. Blue or orange dots indicate MT or BT cells, respectively. The linear approximation curves of MT (blue) and BT (organe) were also shown in the graph.

(D-H) Two-dimensional xy and xz projection images of *Atoh1*-EGFP expression in the developing cochlear epithelium visualized by anti-GFP antibody (grayscale).

It is important to detect low levels of Atoh1 in the xz plane as these are thought to change drastically along this plane from the prosensory domain, a pseudostratified epithelium about five cells thick, into the organ of Corti, two cells thick with HC nuclei on its luminal side and SC nuclei on its basement membrane side. Therefore, two-dimensional xz projection images, as well as two-dimensional xy projection images, were recomposed using confocal z-stack images obtained from whole-mounted, surface-prepared cochlear specimens.

(D-H) xy optical projections. (D'-H') xz single-plane confocal images.

(D, D') E14.5 middle turn. GFP expression was weak and diffuse in the middle turn, and had no gradation along the x-axis or z-axis.

(E, E') E14.5 basal turn. (F, F') E15.5 apical turn. A high level of GFP was observed in cells located at the most medial edge of the GFP-positive area (E, E', F, F').

(G, G') E15.5 middle turn. GFP expression increased in the cells of the lateral prosensory compartment, not only near the luminal side but also near the basement membrane side, along the z-axis.

(H, H') E15.5 basal turn. Strong GFP signals were restricted to cells located near the lumen that were arranged in four rows, suggesting that these GFP-positive cells were differentiating HCs.

bm, basement membrane. Scale bar: D - H', 10 μm.

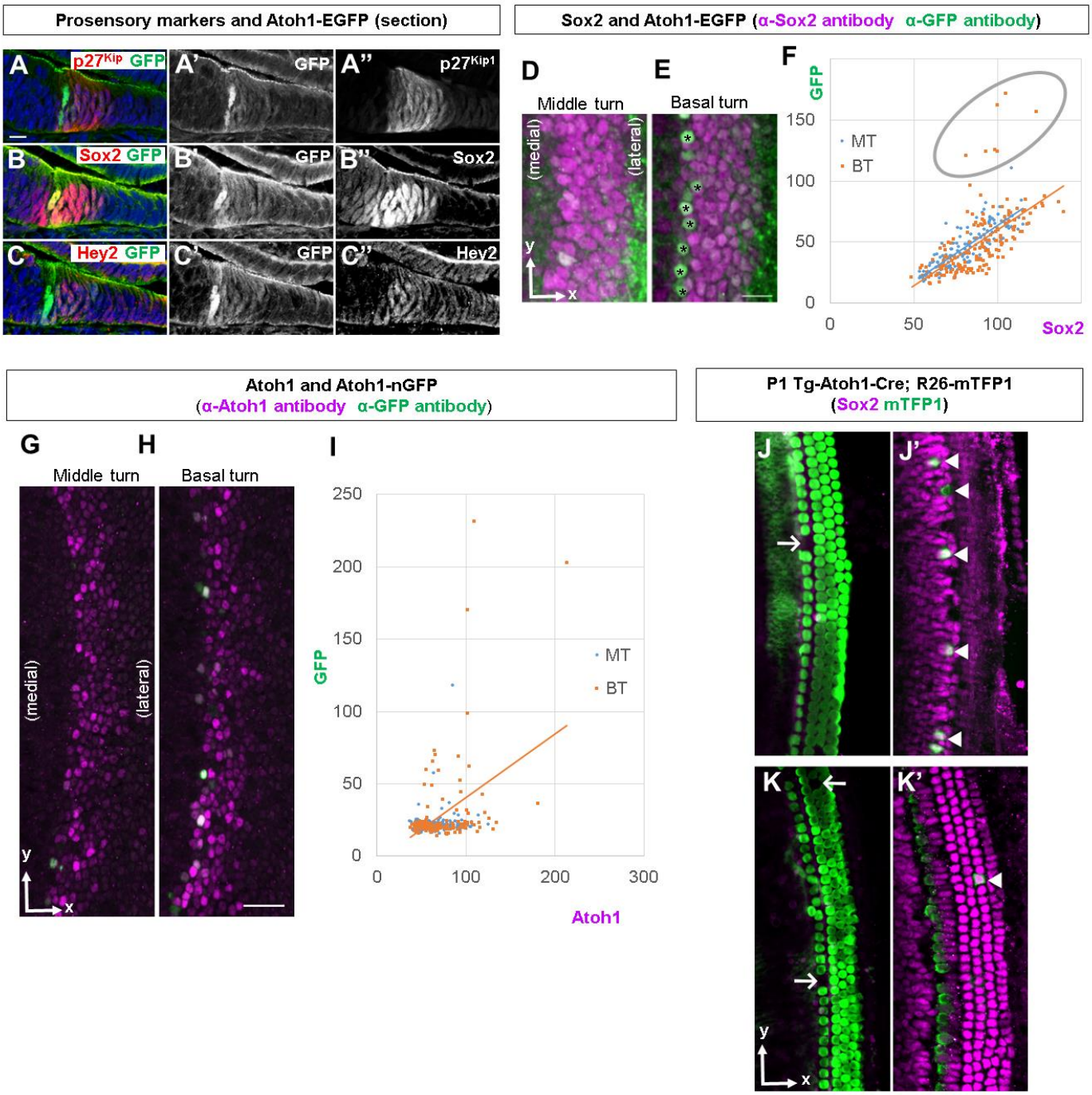

Fig. S2. Atoh1 expression in the developing cochlear epithelium.

(A-C) Weak Atoh1 expression in the prosensory domain.

Immunohistochemical staining for GFP and the prosensory markers p27Kip1, Sox2 and Hey2 in Phase II (E14.5 basal turn) of *Atoh1*-EGFP cochlear mid-modiolar sections.

(A-C) GFP (green), other prosensory markers p27Kip1, Sox2 or Hey2 (magenta), and DAPI (blue).

(A'-C') GFP in gray scale.

(A"-C") p27Kip1, Sox2 and Hey2 prosensory markers in gray scale. Scale bar: A-C, A'-C', A"-C", 10 μm.

(D-F) Weak Atoh1 expression in Phases I and II is correlated with Sox2 expression levels.

GFP and Sox2 expression in E14.5 *Atoh1*-EGFP whole cochlear epithelium visualized by anti-GFP antibody (green) and anti-Sox2 antibody (magenta).

(D) E14.5 middle turn of *Atoh1*-EGFP cochlea, corresponding to phase I. GFP tended to be expressed in the cells that expressed Sox2 more intensely.

(E) E14.5 basal turn of *Atoh1*-EGFP cochlea, corresponding to Phase II. A similar association to that seen in Phase I was observed. Asterisks indicate the cells that express high GFP. Scale bar: D and E, 10 μm.

(F) Relative intensity of Sox2 and GFP in individual cells. MT, middle turn (blue) ; BT, basal turn (orange). A significant positive linear correlation was observed between Sox2 and GFP (MT, $r = 0.828$; BT, $r = 0.607$, $p<0.01$). The linear approximation curves of MT (blue) and BT (orange) were shown in the graph.

The seven points circled with gray lines are the cells indicated in panel E by asterisks, and are outliers from the linear approximation curve as their relative increase in Sox2 was less than that of GFP.

(G-K, J'-K') Atoh1 enhancer becomes active in cells fated to be hair cells, not in the prosensory cells before fate determination.

(G-I) Comparison of *Atoh1*-nGFP reporter with endogenous Atoh1 expression in E14.5 cochlear epithelium.

(G, H) GFP expression in E14.5 cochlear epithelium of *Atoh1*-nGFP mice was compared with endogenous Atoh1 expression by immunohistochemistry, using anti-GFP (green) and anti-Atoh1 (magenta) antibodies. (G) Middle turn corresponding to Phase I. (H) Basal turn corresponding to Phase II. Scale bar: G and H, 20 μm.

(I) Relative intensity of Atoh1 and GFP in individual cells are plotted as blue dots (middle turn, also shown in panel G) and orange dots (basal turn, also shown in panel H). There is a significant positive linear correlation between Atoh1 and GFP of cells in the basal turn (BT) ($r = 0.411$, $p < 0.01$), but a positive linear correlation was not observed in the middle turn (MT) ($r = 0.147$). The linear approximation curves of BT (orange) was shown in the graph.

(J-K, J'-K') Cell lineage detected after Atoh1 enhancer activity. Tg-*Atoh1*-Cre mice, in which the Cre expression is driven by an Atoh1 enhancer element, were crossed with R26-mTFP1 reporter mice so as to detect cell lineage of the same populations labeled by GFP in *Atoh1*-nGFP mice. Double transgenic offspring were harvested at postnatal day 1 and analyzed using antibodies against mTFP (green) and Sox2 (magenta). mTFP1 was detected using an anti-HA antibody.

(J, K) Single plane confocal images in which rows of HC nuclei are apparent. Most HCs stained positively for mTFP1, but mTFP1-negative HCs were occasionally seen (arrows).

(J', K') Single plane confocal images in which rows of Sox2-positive SC nuclei are apparent at the same x-y position as panels J and K. Sox2-positive SCs were mostly mTFP1-negative but some were mTFP1-positive (arrowheads).

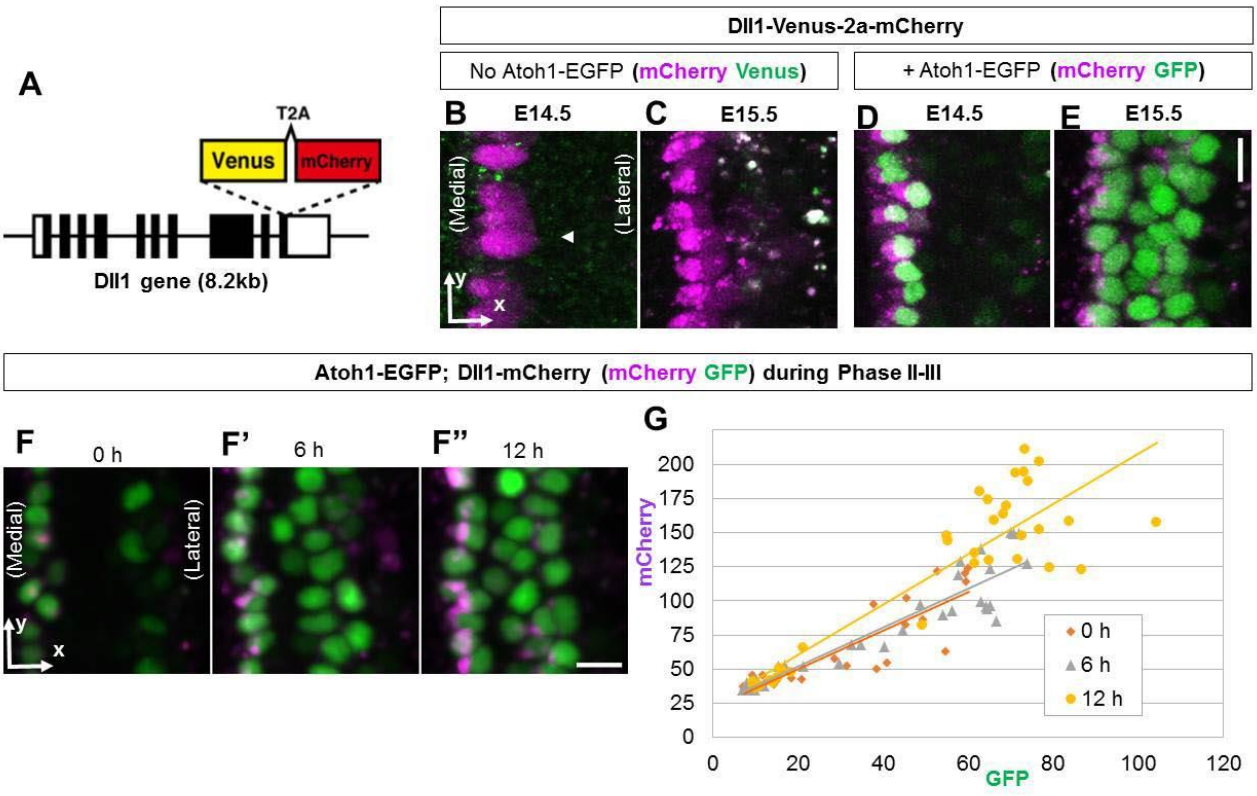

Fig. S3. Visualization of hair cell fate determination using Dll1 C-terminal Venus-T2A-mCherry.

(A) Dll1 C-terminal Venus-T2A-mCherry fusion reporter knock-in construct.

(B-E) GFP imaging is not affected by Venus fluorescence in the double transgenic mice of *Atoh1*-EGFP and Dll1-Venus-2a-mCherry.

Dll1-Venus-T2A-mCherry cochlear explants were analyzed using live imaging; the detection of GFP was not affected by Venus fluorescence in the double transgenic mice carrying *Atoh1*-EGFP and Dll1-Venus-T2A-mCherry.

(B, C) Live imaging of Dll1-Venus-T2A-mCherry cochlear epithelium.

(B) E14.5 basal turn, corresponding to Phase II. mCherry (magenta) was detected in a row of presumptive IHCs. There was little Venus signal (green) in the imaging conditions for GFP detection.

(C) E15.5 basal turn, corresponding to Phase III. mCherry (magenta) was weakly expressed in the lateral compartment. There was little Venus signal (green) in the imaging conditions for GFP detection.

(D, E) Live imaging of Dll1-Venus-T2A-mCherry; *Atoh1*-EGFP cochlear epithelium. The signal of mCherry was derived from Dll1-Venus-T2A-mCherry, and the signal of GFP was thought to be derived from *Atoh1*-EGFP.

(D) E14.5 basal turn. (E) E15.5 basal turn.

(F-F", G) Dll1 is expressed in *Atoh1*-high cells during Phase II-III in *Atoh1*-EGFP;Dll1-mCherry cochlear epithelium.

Atoh1-EGFP; Dll1-mCherry cochlear explants were established at E14.5 and time-lapse imaging was performed.

(F-F”) Two-dimensional xy projection images at 0 h (F), 6 h (F’) and 12 h (F”) from the start of imaging, indicating the transition from Phase II to Phase III.

(G) Relative GFP and mCherry intensity in individual cells.

The number of cells expressing both high GFP and mCherry increased with time. A significant positive linear correlation between Atoh1 and mCherry was observed at all three time points (0 h, $r = 0.893$; 6 h, $r = 0.927$; 12 h, $r = 0.895$, $p < 0.01$), and the linear approximation curves at each time point shown in the graph were similar.

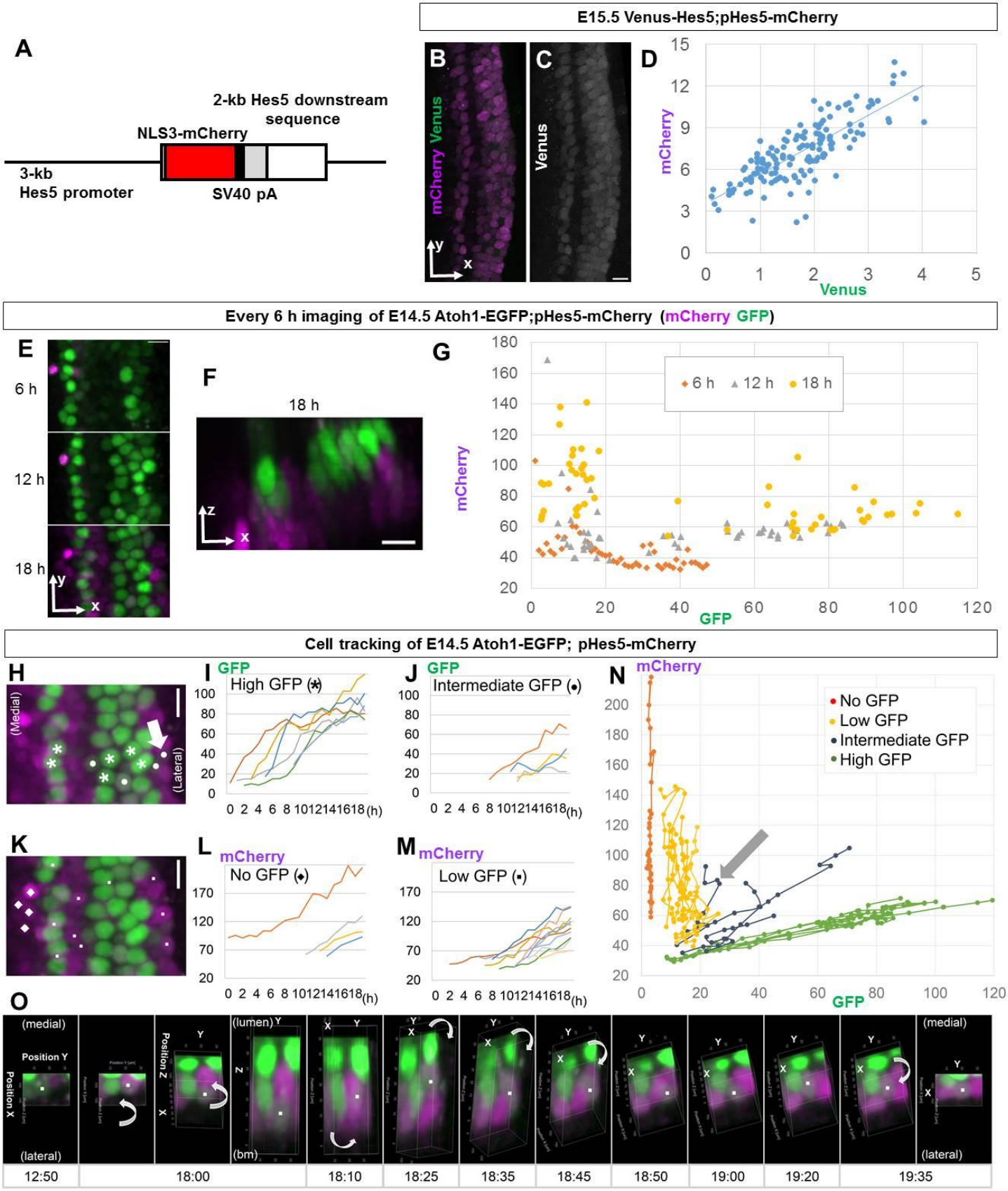

Fig. S4. Live imaging of *Hes5* in the developing cochlear epithelium.

(A-G) Visualization of supporting cell fate determination by pHes5-mCherry line.

(A) pHes5-NLS3-mCherry reporter construct.

(B-D) mCherry expression of pHes5-mCherry cochleae mimics endogenous Hes5 expression.

As immunolabeling for Hes5 was difficult, pHes5-NLS3-mCherry mice were crossed with Venus-Hes5 fusion knock-in mice, in which Venus expression faithfully represents endogenous Hes5 expression (Imayoshi et al., 2013).

(B,C) E15.5 pHes5-mCherry;Venus-Hes5 cochlear epithelium, corresponding to Phase III, expressed both mCherry (magenta in B) and Venus (green in B and grayscale in C), though Venus signal intensity was faint. The fluorescence of mCherry and Venus was captured by confocal microscopy. mCherry expression in the cochlea of pHes5-mCherry embryos mimicked endogenous Hes5 expression and was more readily detectable.

(D) The relative intensity of mCherry and Venus in individual cells. A significant positive linear correlation was observed ($r = 0.788$, $p < 0.01$).

(E-G) Most prosensory cells become either Atoh1-dominant cells or Hes5-dominant cells.

Atoh1-EGFP;pHes5-mCherry cochlear explants were established at E14.5 and time-lapse imaging was performed.

(E) Two-dimensional xy projection images at 6, 12 and 18 h after the start of imaging, covering the transition period from Phase II to Phase III. (F) A snapshot of xz projection (the same view as **Movie 6**) at 18 h. (G) The relative intensity of GFP and mCherry within individual cells. At 6 h, most cells showed low GFP/low mCherry levels; thereafter, two subpopulations of high GFP/low mCherry and low GFP/high mCherry gradually appeared over time. This suggests that most prosensory cells become either Atoh1-dominant cells or Hes5-dominant cells.

(H-O) Cell tracking of *Atoh1*-EGFP;pHes5-mCherry during Phases II-III reveals that neutral cells express intermediate levels of Atoh1 and Hes5 at the end of Phase III

Cells that expressed GFP and/or mCherry in cochlear explants of *Atoh1*-EGFP;pHes5-mCherry embryos at E14.5 were tracked to the end of the experiment at 19 hours, and found to fall into four groups according to GFP intensity: high GFP, intermediate GFP, low GFP and no GFP.

(H) xy projection images at 19 h. GFP (green) and mCherry (magenta). Six cells exhibited high GFP (asterisks), and 4 cells exhibited intermediate GFP (dots). (I) Relative GFP intensity of high GFP cells per hour. As time progressed, the GFP intensity of cells with high GFP levels increased. It indicated that cells with high GFP were committed to an HC fate. (J) Relative GFP intensity of intermediate GFP cells per hour. (K) xy projection images at 19 h. GFP (green) and mCherry (magenta). Ten cells exhibited low GFP (small dots), and four cells exhibited no-GFP (rhombuses). (L) Relative mCherry intensity of no GFP cells per hour. (M) Relative mCherry intensity of low GFP cells per hour. The mCherry intensity of cells with no GFP or low GFP increased. Cells with no or low GFP were thought to be committed to an SC fate. (N) GFP and mCherry intensities of individual tracks. A subpopulation of intermediate GFP cells (blue) were located between two cell subpopulations with high GFP/low mCherry cells (green) and low GFP/high mCherry cells (yellow). This observation suggests that cells with an intermediate GFP level may be “neutral”, and that their fate commitment remains undetermined. **Movies 7 and 8** show a representative neutral cell that corresponds to those arrowed in H, N.

(O) A series of snapshots of **Movie 8**. Arrows indicate the direction to rotate the image. The marked cell is the same as indicated by arrows in H and N, and adjacent to a cell with a high GFP level and a cell with high mCherry level and moves up and down in **Movie 8**.

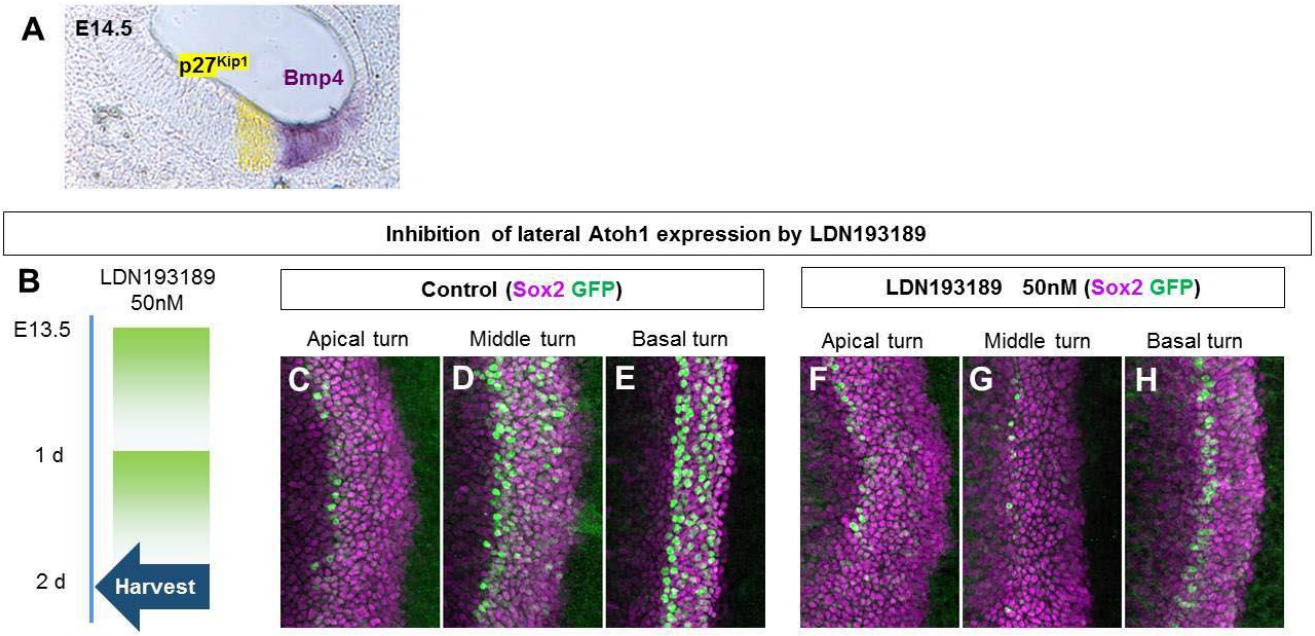

Fig. S5. The effects of Bmp signaling on OHC differentiation.

(A) Bmp4 is expressed in the cochlear epithelium lateral to the prosensory domain.

In situ hybridization of Bmp4 in E14.5 cochlear mid-modiolar sections. Bmp4 is expressed in the cochlear epithelium lateral to p27Kip1-positive prosensory domain.

(B-H) OHC differentiation is suppressed by a Bmp4 signaling inhibitor.

The Bmp4 inhibitor LDN193189 was used to elucidate the Bmp4 signaling pathway in prosensory cells.

(B) The schedule for explant culture establishment, inhibitor LDN193189 administration, and sampling.

(C-H) xy projection images obtained using confocal microscopy. E13.5 *Atoh1*-EGFP cochleae were cultured for 2 days with or without LDN193189, harvested, fixed and used immunohistochemically stained for GFP (green) and Sox2 (magenta).

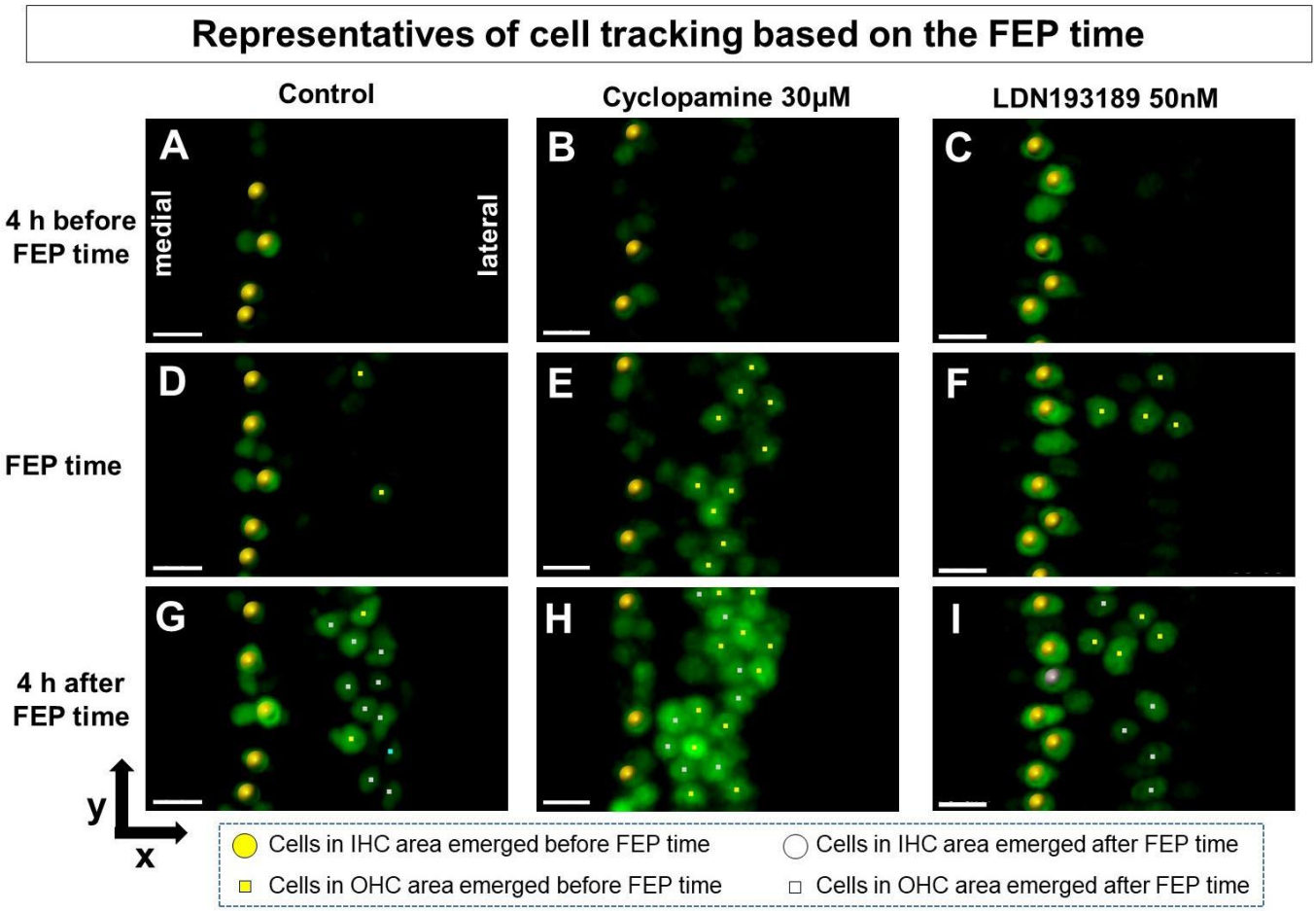

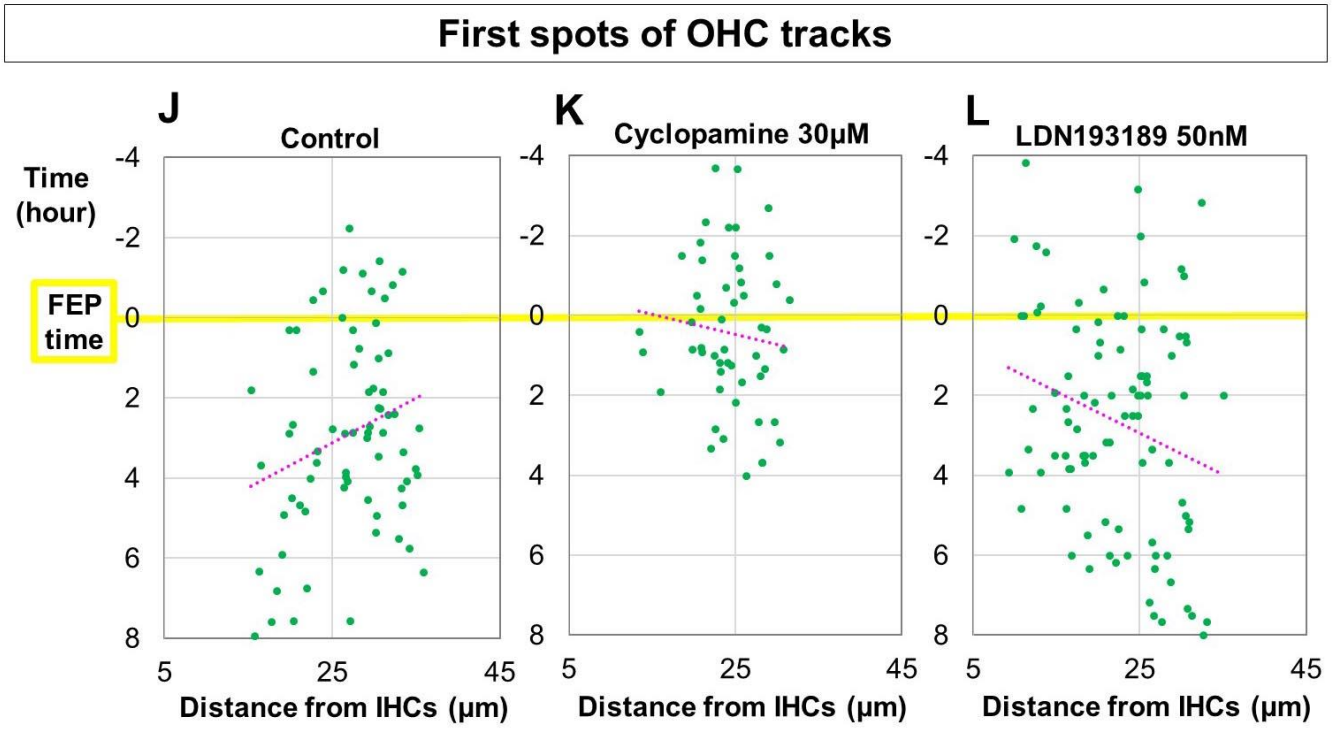

Fig. S6. Effects of Hh inhibitor and Bmp4 inhibitor on Atoh1 expression and OHC patterning.

(A-I) Snapshots of live imaging with Hh inhibitor and Bmp4 inhibitor.

xy projection images of GFP-positive cells in the *Atoh1*-EGFP cochlear explant were tracked from four hours

before the time of FEP. Spheres and squares indicate the cells differentiating into IHCs and OHCs, respectively, and the tracks appeared before the time of FEP are marked by yellow, and those after the time of FEP are white.

(A, D, G) A representative of control experiment. These are the snapshots of **Movie 13**.

(B, E, H) A representative of the experiment with cyclopamine. These are the snapshots of **Movie 14**.

(C, F, I) A representative of the experiment with LDN193189. These are the snapshots of **Movie 15**.

(J-L) The first spots of OHC tracks

Distance between the first spot of each OHC track and mean position of IHCs is calculated, and the distance from IHCs and the time of first OHC spots are plotted. Each of control, cyclopamine and LND193189 group consisted of three time-lapse experiments. A yellow line indicates the time of FEP, and magenta dotted lines are linear approximation curves.

Table S1

Time-lapse imaging conditions

Embryonic day	GFP reporter line	mCherry reporter line	Medicine	Microscope	Total Imaging Time	Time interval (min)	Z-Stack slices	Image size Z (µm)	Scaling Z (µm)	Laser 561nm (%)	Laser 488nm (%)
E14.5	Atoh1-EGFP	Dll1-mCherry	None	LSM780	19h25m	5	25	37.11	1.484	0.1	0.04
E14.5	Atoh1-EGFP	Dll1-mCherry	None	LSM710	20h45m	5	10	42.26	4.700	0.04	0.08
E14.5	Atoh1-EGFP	Dll1-mCherry	None	LSM780	20h50m	5	29	41.56	1.480	0.04	0.1
E14.5	Atoh1-EGFP	pHes5-mCherry	None	LSM780	19h35m	5	27	40.08	1.484	0.02	0.05
E14.5	Atoh1-EGFP	pHes5-mCherry	None	LSM780	22h4m	5	27	40.08	1.484	0.02	0.05
E14.5	Atoh1-EGFP	pHes5-mCherry	None	LSM780	24h54m	5	27	40.08	1.484	0.02	0.05
E13.5	Atoh1-EGFP	R26-H2B-mCherry	None	LSM780	20h0m	5	20	38.66	1.933	0.06	0.5
E14.5	Atoh1-EGFP	pHes5-mCherry	None	LSM780	26h53m	10	6.45	44.4	1.138	0.15	0.04
E13.5	Atoh1-EGFP	pHes5-mCherry	Cyclopamine 30uM	LSM780	45h9m	5	25	31.65	1.266	0.07	0.07
E14.5	Atoh1-EGFP	Dll1-mCherry	Cyclopamine 30uM	LSM710	23h12m	6	28	42.2	1.507	0.07	0.04
E14.5	Atoh1-EGFP	Dll1-mCherry	Cyclopamine 30uM	LSM780	24h10m	5	28	38.84	1.439	0.1	0.05
E14.5	Atoh1-EGFP	Dll1-mCherry	Cyclopamine 30uM	LSM880	20h50m	5	28	40.2	1.489	0.09	0.3
E14.5	Atoh1-EGFP	Dll1-mCherry	Cyclopamine 30uM	LSM880	20h50m	5	26	37.19	1.488	0.09	0.3
E14.5	Atoh1-EGFP	pHes5-mCherry	Cyclopamine 30uM	LSM780	19h20m	10	30	40.89	1.410	0.08	0.02
E14.5	Atoh1-EGFP	pHes5-mCherry	Cyclopamine 30uM	LSM880	47h50m	10	37	43.2	1.200	0.06	0.018
E13.5	Atoh1-EGFP	pHes5-mCherry	LDN 50nM	LSM880	17h9m	5	25	34.47	1.379	0.1	0.2
E14.5	Atoh1-EGFP	Dll1-mCherry	LDN 50nM	LSM780	41h30m	5	28	40.18	1.488	0.1	0.05
E14.5	Atoh1-EGFP	Dll1-mCherry	LDN 50nM	LSM780	44h50m	5	27	37.04	1.425	0.09	0.04
E14.5	Atoh1-EGFP	Dll1-mCherry	LDN 50nM	LSM780	41h30m	10	30	41.91	1.445	0.09	0.02
E14.5	Atoh1-EGFP	-	LDN 50nM	LSM780	44h50m	10	30	41.89	1.444	-	0.018
E14.5	Atoh1-EGFP	-	LDN 50nM	LSM880	53h50m	10	38	44.4	1.200	-	0.018
Average					**29h33m**	**6.5**	**26.3**	**39.92**	**1.589**	**0.07**	**0.098**

Movies

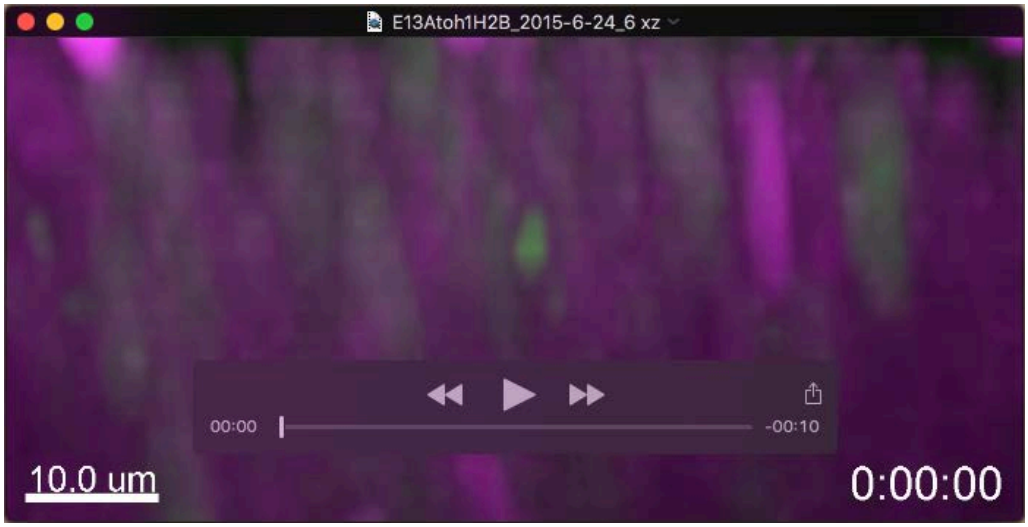

Movie 1

The view shown in **Fig. 3B-G**, containing xz projection images of the time-lapse experiment. The area of the x, y and z direction is 76.1 µm, 38.7 µm and 64.6 µm, respectively.

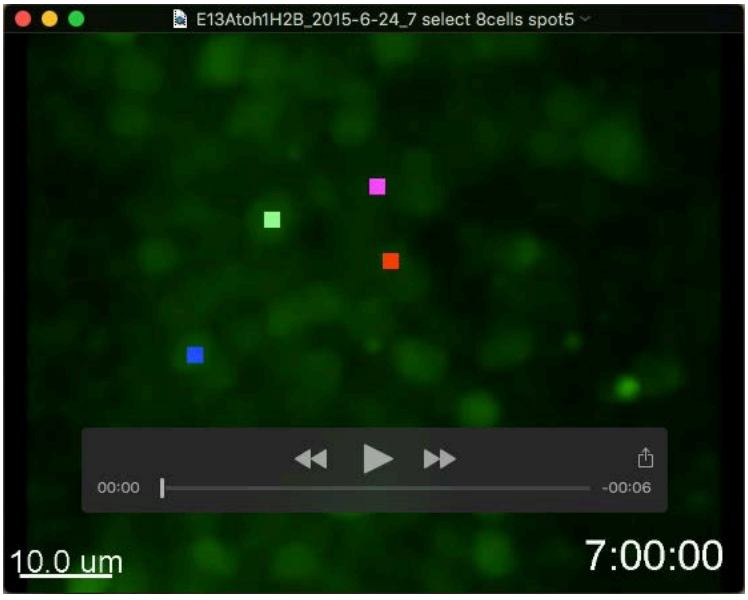

Movie 2

xy projection images of the time-lapse experiment using E13.5 *Atoh1*-EGFP;R26-H2B-mCherry cochlear explants between 7 and 19 h. Each color indicates cells 1–8, and is the same as in **Fig. 3L**.

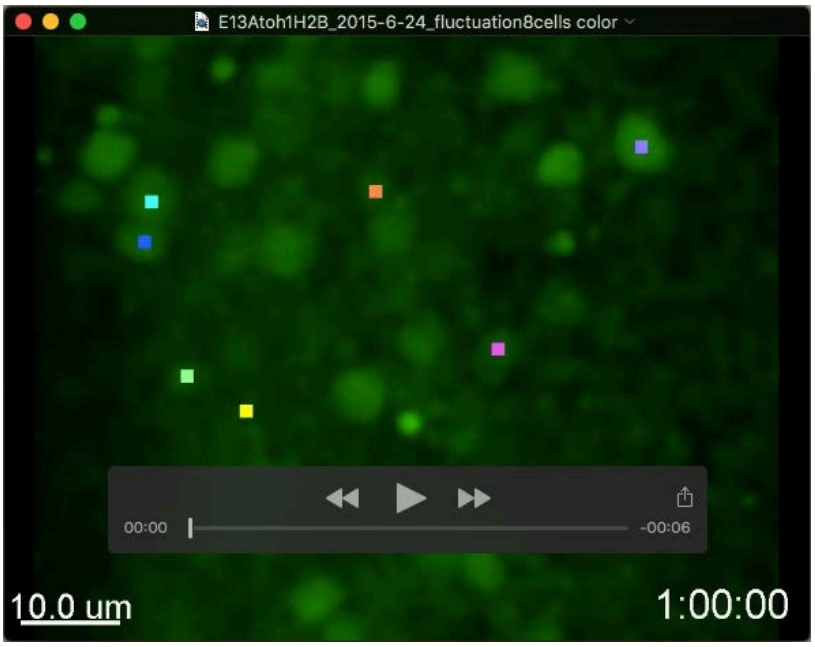

Movie 3

xy projection images of the time-lapse experiment using E13.5 *Atoh1*-EGFP;R26-H2B-mCherry cochlear explant**s** between 1 and 13 h. Each color of the points indicates cell**s** 9–16 and is the same as in **Fig. 3P**.

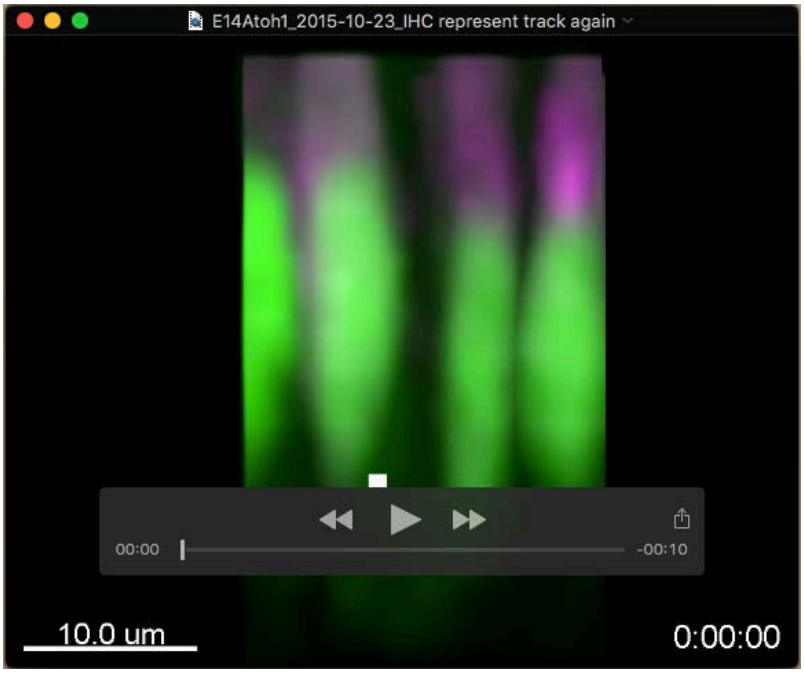

Movie 4

Two-dimensional yz projection images viewed from the medial side (the orientations are denoted by arrows between **Fig. 4A and 4A'**), focusing on presumptive IHCs indicated by white dots.

The depth of the x direction is 18.8 μm

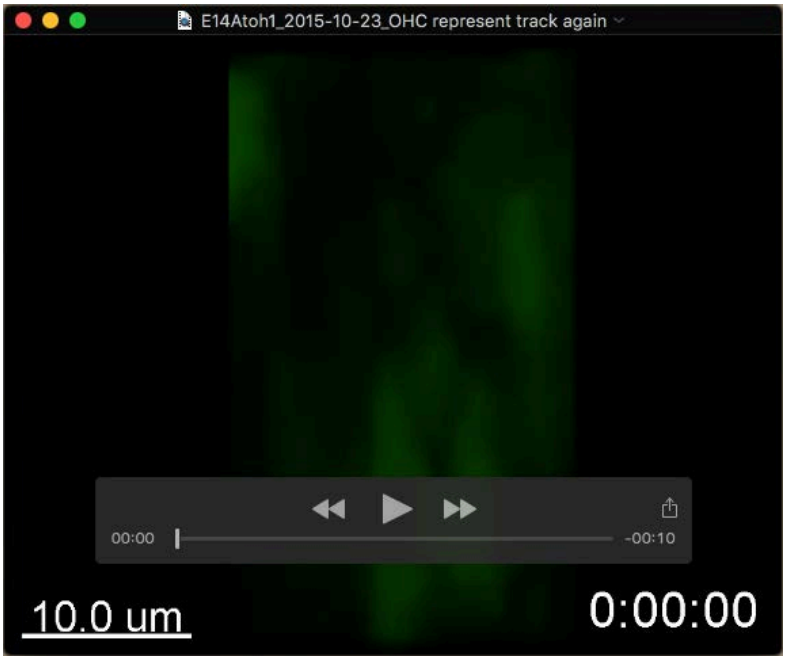

Movie 5

Two-dimensional yz projection images viewed from the lateral side (the orientations are denoted by arrows between **Fig. 4A and 4A'**), focusing on presumptive OHCs indicated by cyan dots.
The depth of the x direction is 26.3 μm

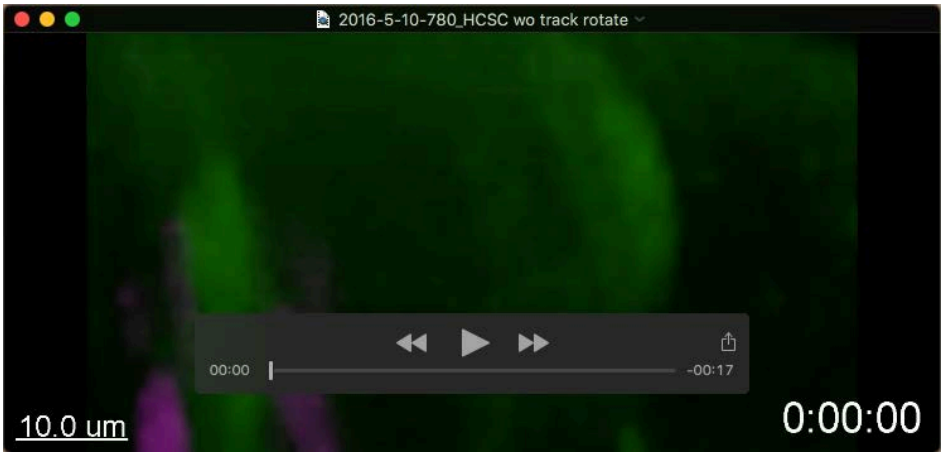

Movie 6

Two-dimensional xz projection images from 0 to 18 h; the image contrast of the GFP intensity was reduced twice, at 6 h and 12 h (**Supplemental Fig. 4F**). The depth of the y direction is 46.1 μm.

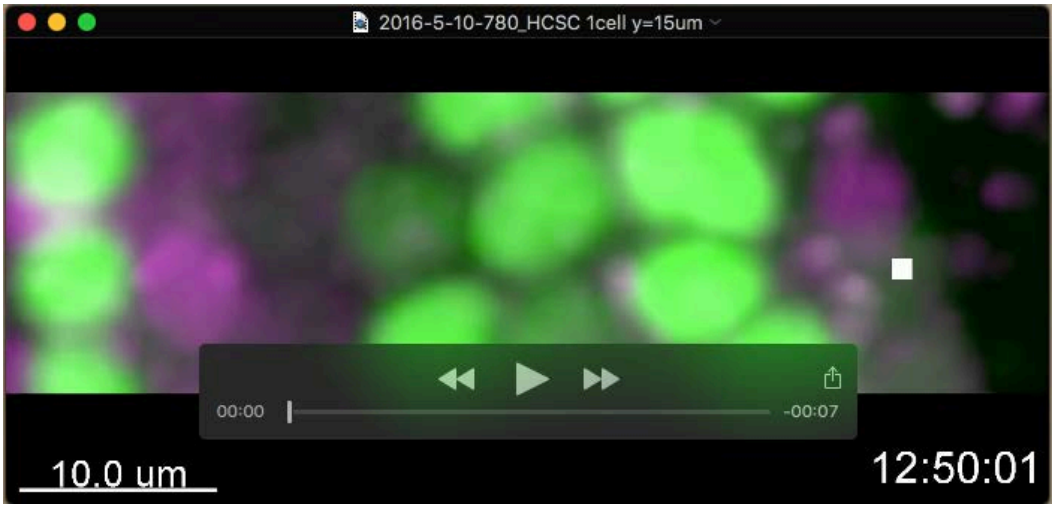

Movie 7

xy projection images of a representative neutral cell, which corresponds to the arrows in **Supplemental Fig. 4H**. The marked cell is adjacent to a high GFP and high-mCherry cell and moves up and down in Movie 8. The depth of the z direction is 41.8 μm.

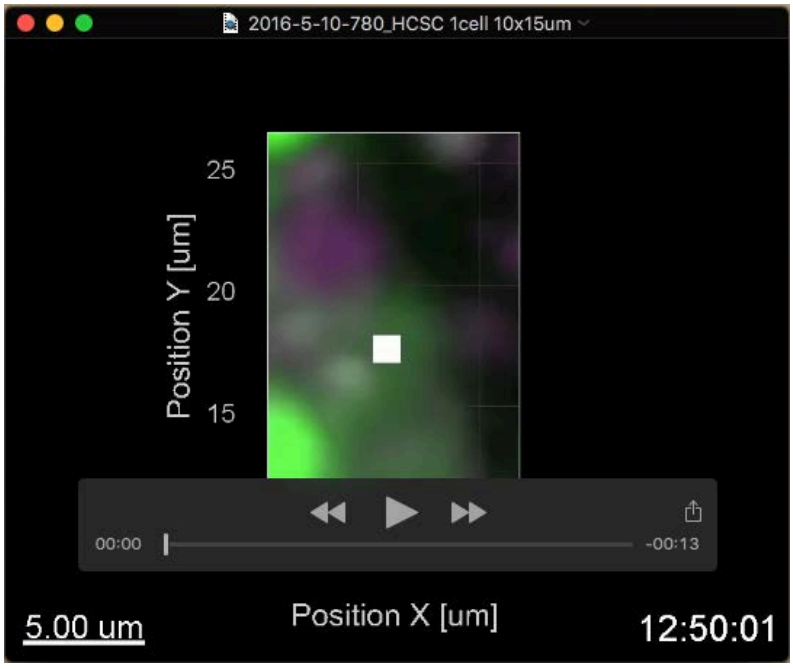

Movie 8

A magnified image of **Movie 7** containing a representative neutral cell, which corresponds to the arrows in **Supplemental Fig. 4O**. This movie is systematically rotated to maintain the marked cell in the foreground.

Movie 9

xy projection images of the time-lapse experiment using E14.5 *Atoh1*-EGFP cochlear explants. The snapshots of Movie 10 are shown in Fig.5D-N. Without color grouping.

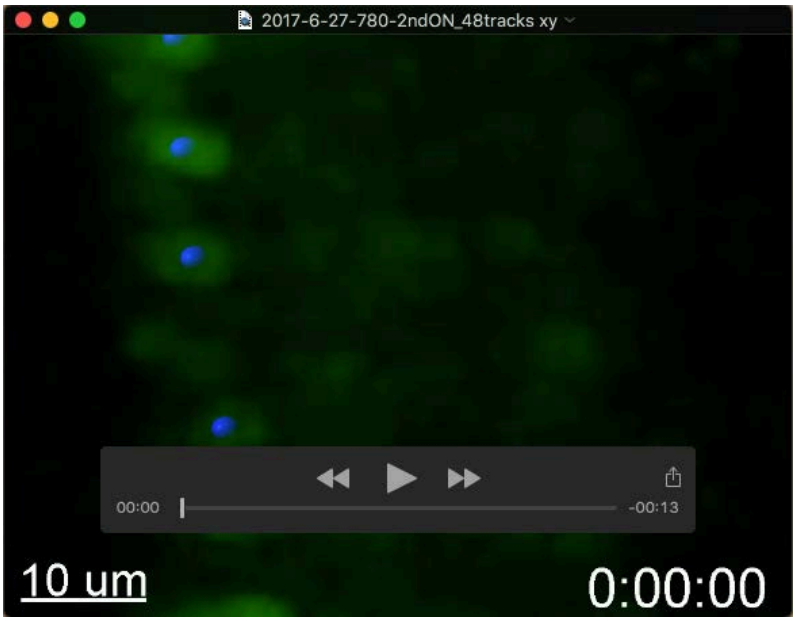

Movie 10

xy projection images of the time-lapse experiment using E14.5 *Atoh1*-EGFP cochlear explants. The snapshots of Movie 10 are shown in Fig.5D-N. With color grouping.

Movie 11

xz projection images of the time-lapse experiment using E14.5 *Atoh1*-EGFP cochlear explants. The snapshots of Movie 12 are shown in Fig. 5D'-N'. Without color grouping.

Movie 12

xz projection images of the time-lapse experiment using E14.5 *Atoh1*-EGFP cochlear explants. The snapshots of Movie 12 are shown in Fig. 5D'-N'. With color grouping.

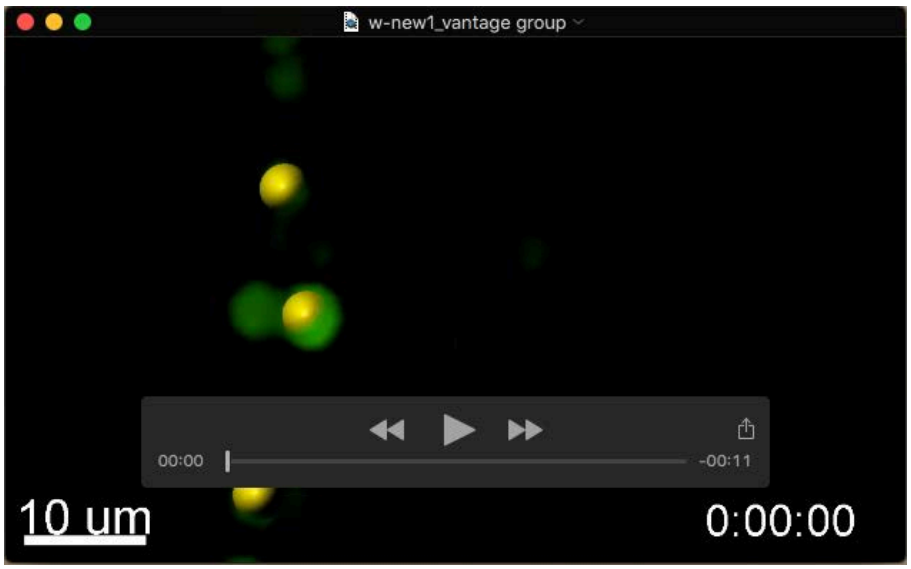

Movie 13

xy projection images of the time-lapse experiment using E14.5 *Atoh1*-EGFP cochlear explants, which corresponds to Fig. S6A, D, G.

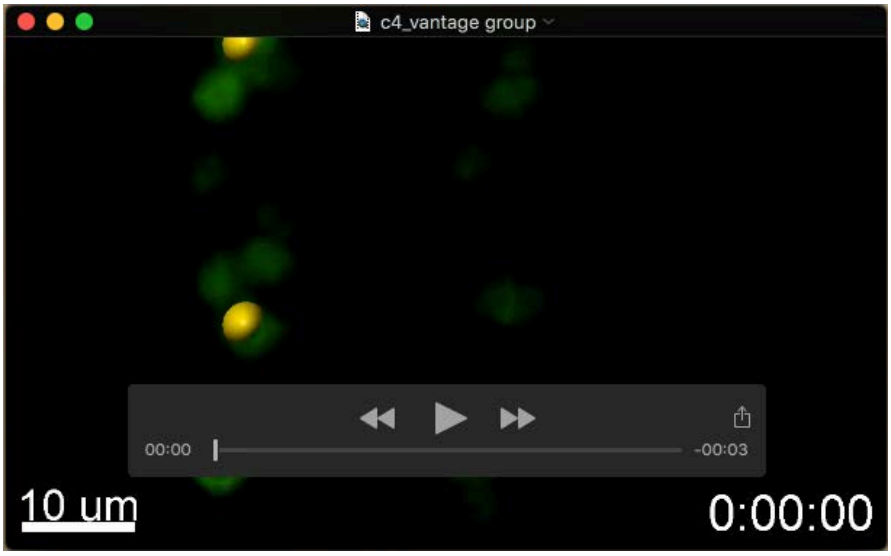

Movie 14

xy projection images of the time-lapse experiment using E14.5 *Atoh1*-EGFP cochlear explants with cyclopamine, which corresponds to Fig. S6B, E, H.

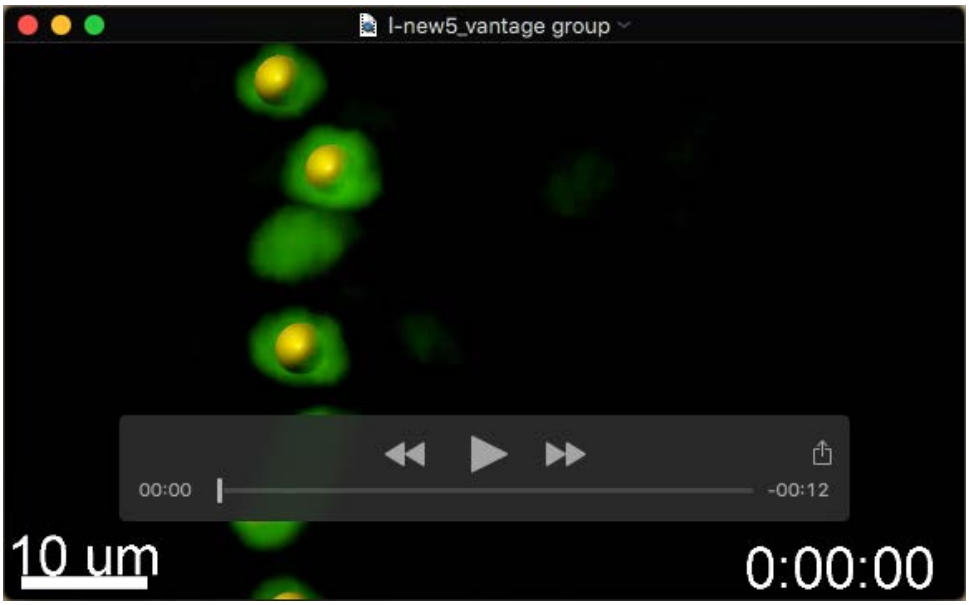

Movie 15

xy projection images of the time-lapse experiment using E14.5 *Atoh1*-EGFP cochlear explants with LDN193189, which corresponds to Fig. S6C, F, I.